Proceedings of FUELCELL2006
The 4th International Conference on FUEL CELL SCIENCE, ENGINEERING and TECHNOLOGY
June 19-21, 2006, Irvine, CA

FUELCELL2006-97011

ROBUST DESIGN TECHNIQUES FOR EVALUATING FUEL CELL THERMAL PERFORMANCE

Kenneth J. Kelly[1], Gregory C. Pacifico[2], Michael Penev[3], Andreas Vlahinos[4]

[1]National Renewable Energy Laboratory, Golden, CO 80401, USA, kenneth_kelly@nrel.gov
[2]Plug Power, Inc., Latham, NY 12110, USA, greg_pacifico@plugpower.com
[3]Plug Power, Inc., Latham, NY 12110, USA, michael_penev@plugpower.com
[4]Advanced Engineering Solutions, LLC**,** Castle Rock, CO 80108, USA andreas@aes.nu

ABSTRACT

The National Renewable Energy Laboratory (NREL) and Plug Power Inc. have been working together to develop fuel cell modeling processes to rapidly assess critical design parameters and evaluate the effects of variation on performance. This paper describes a methodology for investigating key design parameters affecting the thermal performance of a high temperature, polybenzimidazole (PBI)-based fuel cell stack. Nonuniform temperature distributions within the fuel cell stack may cause degraded performance, induce thermo-mechanical stresses, and be a source of reduced stack durability. The three-dimensional (3-D) model developed for this project includes coupled thermal/flow finite element analysis (FEA) of a multi-cell stack integrated with an electrochemical model to determine internal heat generation rates. Sensitivity and optimization algorithms were used to examine the design and derive the best choice of the design parameters. Initial results showed how classic design-of-experiment (DOE) techniques integrated with the model were used to define a response surface and perform sensitivity studies on heat generation rates, fluid flow, bipolar plate channel geometry, fluid properties, and plate thermal material properties. Probabilistic design methods were used to assess the robustness of the design in response to variations in load conditions. The thermal model was also used to develop an alternative coolant flow-path design that yields improved thermal performance. Results from this analysis were recently incorporated into the latest Plug Power coolant flow-path design. This paper presents an evaluation of the effect of variation on key design parameters such as coolant and gas flow rates and addresses uncertainty in material thermal properties.

INTRODUCTION

Engineers at the National Renewable Energy Laboratory (NREL) have been working to adopt advanced design processes and apply them in the development of energy efficient technologies. Often the industries developing these technologies do not have the dedicated engineering and analytical resources to fully develop the necessary integrated design processes. NREL has worked closely with some of these partners over the past several years to apply virtual prototyping methods that couple structural, thermal, and fluid flow simulations to variational techniques, advanced design optimization, and quality and performance goals. In the past two years, the NREL team has used this expertise in collaboration with Plug Power Inc. to advance optimal design methodologies for fuel cells and improve product development time and costs by reducing the number of physical prototypes and laboratory tests required. This collaboration is helping to overcome technical barriers, reduce fuel cell development time and costs, and drive innovation. The objective of this project was to develop a fuel cell stack thermal modeling process to assess design sensitivity on fuel cell thermal performance and assist in the development of improved heat transfer characteristics.

Nonuniform temperature distributions within the fuel cell stack may cause degraded performance, induce thermo-mechanical stresses, and be a source of reduced stack durability. The project described here involved coupling Plug Power's electrochemical model with a 3-D thermal/fluid finite element analysis (FEA) model developed by NREL. The electro-

chemical model was used to predict a nonuniform heat generation map within the membrane electrode assembly (MEA). This heat generation map was then processed and applied to the thermal/flow FEA model that predicts 3-D plate, fluid, and membrane temperatures. The membrane temperatures were fed back into the electrochemical model and the process was repeated until convergence was achieved. The thermal/flow model uses pipe flow elements for rapid analysis of the 3-D stack's thermal performance. The modeling process described here demonstrates the integration of design-of-experiment (DOE) and probabilistic design techniques to perform sensitivity and variation studies on fuel cell heat generation rates, fluid flow, bipolar plate channel geometry, fluid properties, and plate thermal material properties.

NOMENCLATURE

CAD – computer-aided design
CAE – computer-aided engineering
CCD – central composite design
DOE – design of experiments
FEA – finite element analysis
MEA – membrane electrode assembly
NREL – National Renewable Energy Laboratory
PBI – polybenzimidazole
PDM – probabilistic design methods
3-D – three dimensional

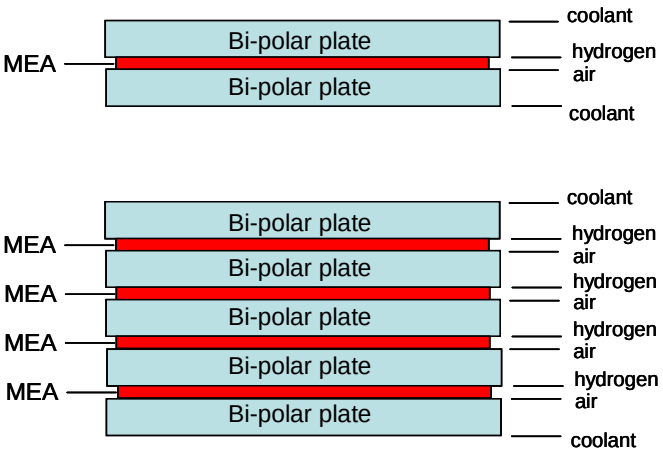

Figure 1. Single-cell and four-cell stack schematic

TECHNICAL APPROACH

A thermal FEA model of Plug Power's high-temperature polybenzimidazole (PBI)-based stack was built using actual CAD geometry of the bipolar plates, fluid flow channels, and material properties supplied by Plug Power. Initial FEA modeling was carried out on a single-cell (two bipolar plates, MEA, and insulation) model. A second FEA model of a four-cell stack was then developed and incorporated into the modeling process. Schematic diagrams of the single-cell and four-cell stack are shown in Figure 1. A key thermal design consideration is the number of cells per cooler. The single-cell model has one full cooler per cell and the four-cell model has four cells per cooler. Note that two-cell and eight-cell designs can also be analyzed using the same models by deleting one of the coolers and applying symmetry expansion to single-cell and four-cell models respectively.

Images from the two FEA models are shown in Figure 2. The solid components of the fuel cell were modeled using 8-node 3-D solid tetrahedral elements for thermal FEA. The fluids (hydrogen, air, and coolant) were modeled with coupled thermal-fluid pipe elements in ANSYS. Convection heat transfer between the solid and the hydrogen, air, and coolant pipes was modeled using convection surfaces and film coefficients calculated from the fluid flow, channel geometry, and fluid physical properties.

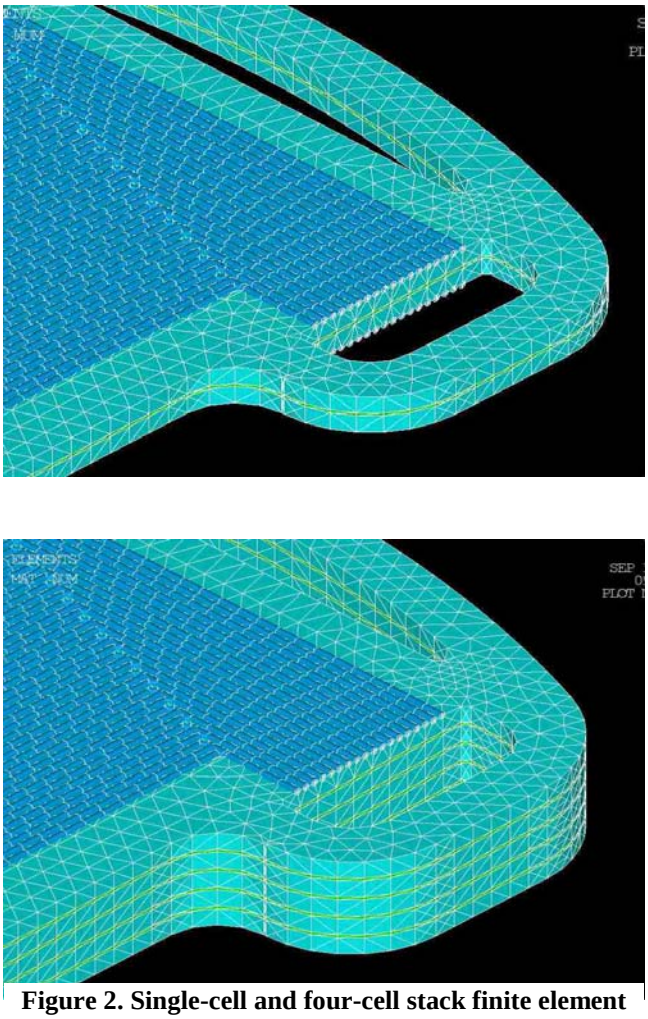

Figure 2. Single-cell and four-cell stack finite element models

The ANSYS pipe element is a 3-D element with the ability to conduct heat and transmit fluid between its two primary

nodes [1]. Heat flow is due to conduction within the fluid and the mass transport of the fluid. Convection is accounted for using additional surface elements. The film coefficient between the surface elements and the pipes is related to the fluid flow rate. Figure 3 shows the network of pipe elements for air, hydrogen, and coolant for the single-cell stack. Figure 4 shows the pipe elements, convection surface elements, and connecting elements between the pipe nodes and the convection surfaces elements.

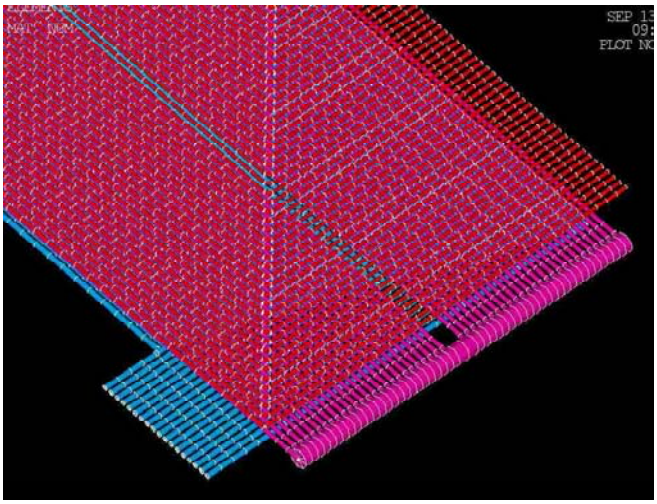

Figure 3. Network of pipe elements, coolant (red), hydrogen (magenta), air (cyan)

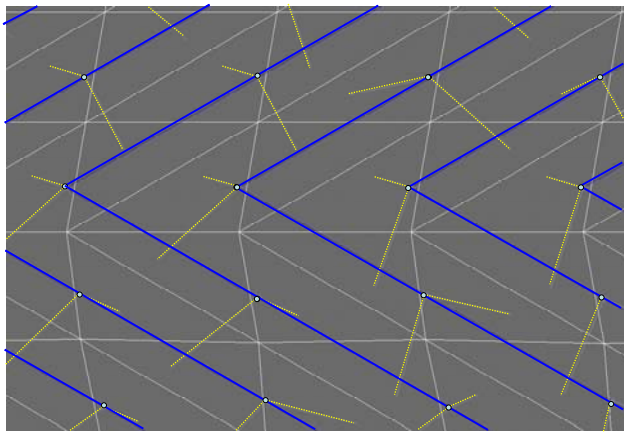

Figure 4. Convection elements (yellow) connect pipe elements (blue) to surface elements (grey)

The use of pipe elements allowed us to model heat transfer between the solids and fluids without detailed computational fluid dynamics (CFD) within the flow channels. This approach assumes uniform flow through the channel cross-section, and allows rapid solutions that can be used to assess relative impacts as well as sensitivity studies and the effects of load and material variations by integrating the model with DOE techniques and probabilistic design methods. Solutions of the single-cell stack model were obtained in a few minutes. This allows many design iterations to be evaluated rapidly. By comparison, similar CFD analyses that model actual flow channel geometry on real-world fuel cell designs may require billions of finite elements, intensive computational power, and many hours (even days) to converge on a single solution.

The thermal FEA model developed here requires internal heat generation at the MEA as an input. Two possible modeling approaches for internal heat generation were evaluated. The first was to use an average heat generation rate and apply it uniformly across the MEA. A second approach was to obtain a nonuniform "map" of the heat generation rates based on an electrochemical model of the cell performance. At the time of this study, Plug Power used an internally developed, proprietary spreadsheet model to predict current density and heat generation rates based on an input temperature map. The spreadsheet model requires a temperature map as input and iterates until a converged solution is achieved. An output from this model is a nonuniform map of heat generation rates along the X and Y coordinates of the MEA. The predicted heat generation map (as shown in Figure 5) was then used as input into the stack thermal FEA model.

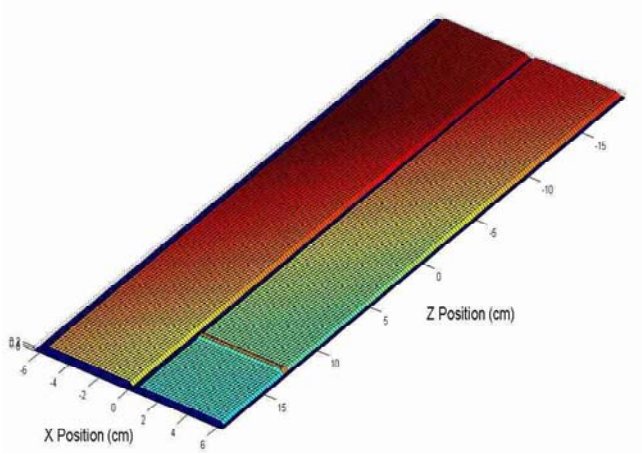

Figure 5. Nonuniform heat generation map

The temperature map from the spreadsheet model included 9000 heat generation points with an X-Y discretization of approximately 2 mm. The FEA mesh included approximately 4500 nodes with discretization between 3 mm and 3.5 mm. A Matlab script was used for the preliminary step of interpolating the predicted heat generation map from the electrochemical model to the FEA model nodal coordinates. The interpolated nonuniform heat generation rates were then applied to the thermal FEA model and solved for the resultant temperature at the nodes. These temperatures were then interpolated back to the spreadsheet grid and compared to the initial temperature

inputs. The overall process (electrochemical model, data processing, and thermal FEA) was repeated until adequate convergence was achieved. A diagram of the overall process and an example of the process convergence are shown in Figure 6 and Figure 7 respectively. The overall process converged to within a root mean square value of 1 x 10^{-4} root mean square after four iterations.

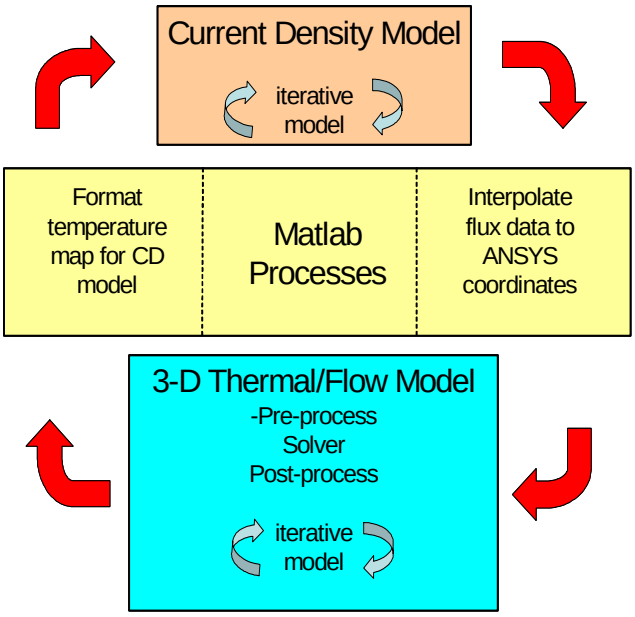

Figure 6. Analysis process integration

The next steps were to develop a parametric modeling process, perform design space investigations using design-of-experiment (DOE) techniques, and then evaluate the effect of load variations using probabilistic design methods (PDM). These steps required a fast, flexible, and robust model to converge on solutions over a wide variety of input levels. Both the DOE study and the PDM analysis required a parametric analysis file to perform the following functions:

1. Build the model parametrically based on the range of input variables,
2. Calculate input values that are altered by varying design parameters (e.g., inlet flow velocities based on updated channel geometries),
3. Assign material properties based on the input conditions,
4. Apply updated boundary conditions,
5. Obtain the solution, and
6. Retrieve output data from the model and calculate output performance parameters.

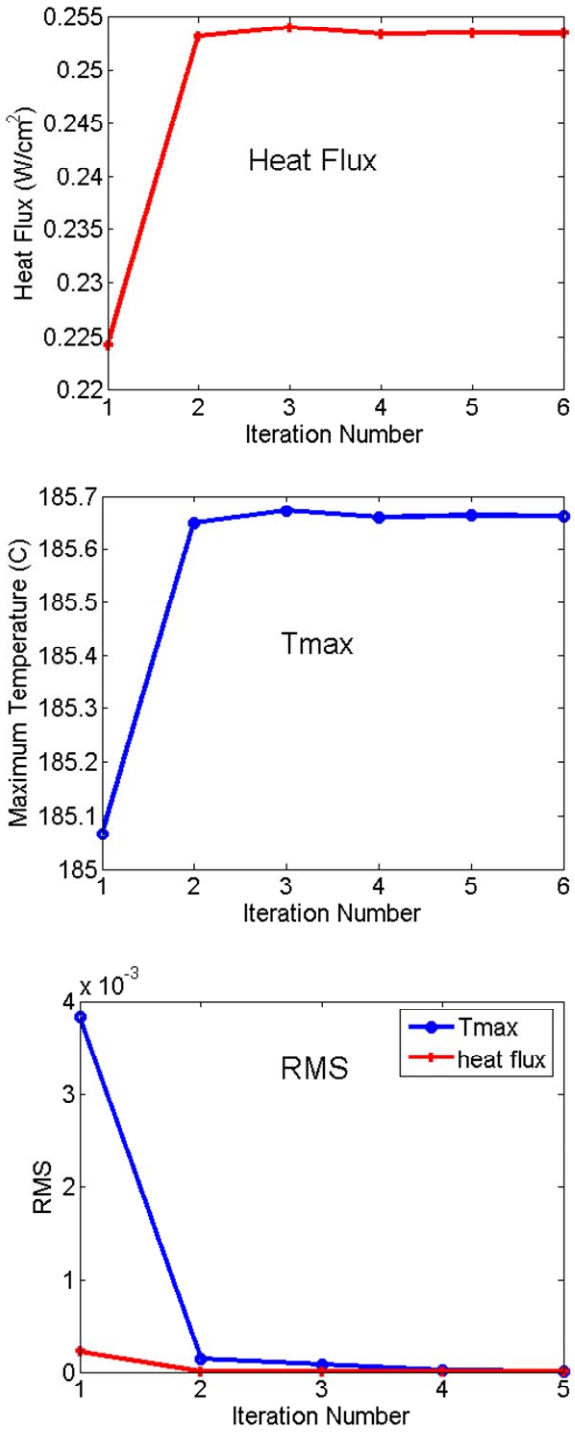

Figure 7. Process convergence example

The output thermal performance variables chosen for this study included: maximum MEA temperature, temperature distribution across the MEA, and coolant pressure drop.

The DOE study required the following additional process steps:

1. Define the design variables and ranges to be studied (see Table 1 in the Results section).
2. Define the output performance parameters to be investigated. Here we chose the maximum MEA temperature ($T_{max\text{-}MEA}$), the temperature differential across the MEA surface (dT_{MEA}), and the coolant pressure drop ($dP_{coolant}$) as output performance measures.
3. Select an experimental design based on the model solution time – such as full factorial, partial factorial, and Taguchi screening approaches [(2)]. For this study, full- and half-factorial approaches were used for the final analysis because the simulation time was relatively short (several minutes). A more efficient three-level Taguchi L18 screening design was also used early in the analysis to help choose the variables to be included in the study.
4. Set up and run the DOE loop using the parametric analysis file.
5. Develop a polynomial fit of the output variables using regression techniques.
6. Evaluate input parameter sensitivities using Pareto charts and sensitivity analysis.

The final major step that we used in the overall analysis process was to setup and perform a PDM analysis to evaluate the effect of load variations on the system thermal performance. The PDM analysis included the following steps:

1. Define the random input variables and ranges to be studied. For the PDM analysis the input parameters were specified by a mean value, standard deviation, and statistical distribution of the inlet coolant temperature, heat generation, and coolant pressure drop. Gaussian input variable distributions were specified with the nominal design value for the mean and a total random variation range of +/- 5% for each input variable.
2. Define the random output performance parameters to be investigated. Tmax-MEA and the dTMEA were chosen as output performance measures.
3. Select a PDM design tool or method, such as Monte-Carlo or response surface analysis. A response surface methodology was used here using a central composite design (CCD) [(2)].
4. Set up and run the PDM loop using the parametric analysis file.
5. Fit the response surface using a regression technique – here we used forward step-wise regression.
6. Evaluate the quality of the response surface with statistical measures such as the R^2 value and standard error.
7. Develop statistical distribution of the output variables based on the input distributions.
8. Evaluate the results.

PDM analysis results can be evaluated with histograms showing the output performance distributions, scatter charts, comparison to upper and lower control specifications, and with reference to sigma quality levels.[(3,4,5,6)]

With a fast and flexible model, DOE and PDM studies of this type can be used to evaluate hundreds of design cases and input variations early in the design process. This can help us define critical design parameters and understand the effects of input variations and uncertainty. Results of the analyses can be used to guide technology development decisions, contribute to manufacturing tolerance specifications, streamline experimental programs, and reduce the number of prototypes that are built and tested.

RESULTS

We performed an initial thermal analysis with the four-cell stack FEA model to determine the relative effects of using the nonuniform heat generation rates predicted by the Plug Power model versus applying an equivalent average uniform heat generation rate within the MEA. This analysis was performed to decide whether the nonuniform heat generation model would be required in future analyses.

Temperature profiles for the four-cell stack are shown in Figure 8. This figure shows the relative temperature profile of the MEA for the uniform and nonuniform heat generation cases. A noticeable difference in the temperature profiles was observed for these two cases. Next, a histogram of the temperature distribution across the MEA surface was generated to compare the two cases in more detail. A similar set of analyses was also run for uniform and nonuniform heat generation with reversed coolant flow directions (i.e., switching the inlet and outlet conditions). Figures 8 and 9 show the temperature distributions for the uniform and nonuniform (or "mapped") heat generations. While the overall average temperature of the MEA was the same for the uniform and nonuniform heat generation cases, the shape of the distribution (e.g., location of maximum temperature regions) and the temperature differential ($T_{max} - T_{min}$) were significantly different. From these analyses, we decided to use the mapped heat generation for all future runs.

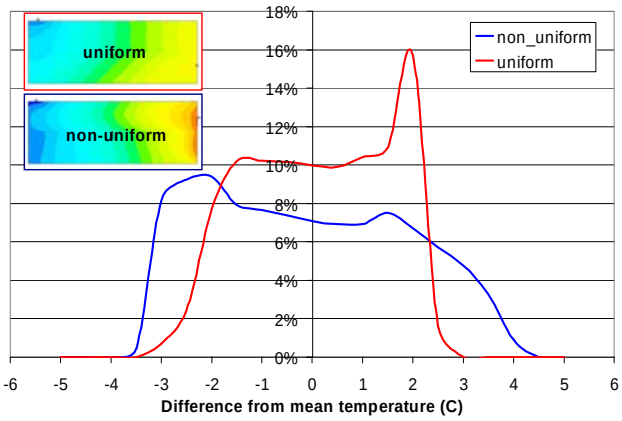

Figure 8. MEA temperature distributions for uniform and nonuniform heat generation

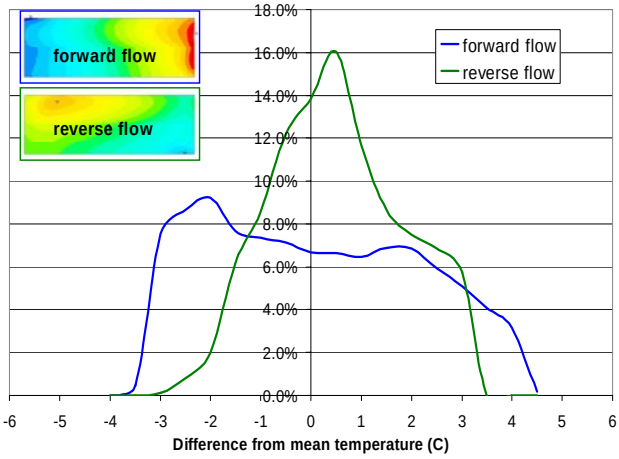

Figure 9. MEA temperature distributions for forward and reverse coolant flow

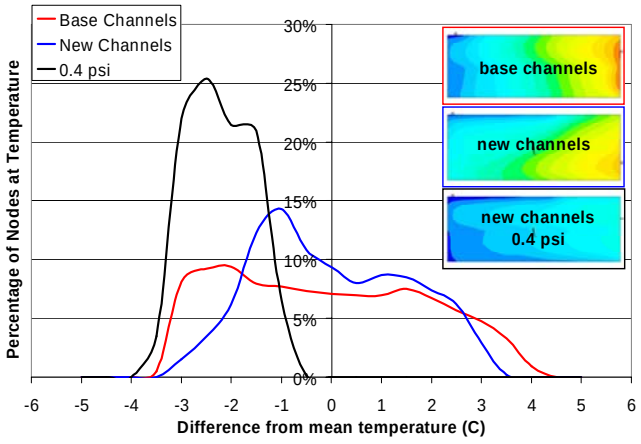

Figure 10. MEA temperature distributions for base and new coolant channel designs

Based on the results from the previous analyses, NREL proposed an alternative coolant flow-path design. The key features of the alternative coolant flow-path design include: a more direct path to the high-temperature region of the membrane, weighting of the spacing of coolant flow channels based on the shape of the nonuniform heat generation map, and a significantly shorter coolant flow path. The results from a thermal analysis of the new design are summarized in the temperature distributions shown in Figure 10. Three temperature distributions are shown. The first is the base case, the second shows the new coolant channels with the same mass flow rate as the base case, and the third shows the new channels with the same coolant pressure drop (0.4 psi) as the base case. Since the alternative design has a significantly shorter flow path, the coolant flow rate was higher for the same pressure drop (i.e., more flow for the same required pumping power). Figure 10 shows an improved temperature distribution for the alternative coolant flow path (new channels). For the same coolant pressure drop, the overall average MEA temperature was approximately 1% lower than the base case, and the temperature differential across the surface of the MEA was 60% lower than the base case. Design concepts from this analysis were recently incorporated into the latest Plug Power coolant flow-path design.

The next step in the analysis process was to determine the relative impact on thermal performance for a set of stack design parameters. To do this, we conducted a series of simulations using DOE techniques with the design parameters and ranges shown in Table 1. The percentages indicate the extent to which the parameters were varied from their nominal setting. The internal heat generation was included as a design parameter to show its effect on thermal performance, but was varied less than the other parameters since it is not as easily controlled. Some values such as the plate and coolant thermal conductivity require a change in materials to achieve the range.

Table 1. Design Parameters and Ranges for Design of Experiments

Design Parameter	Range Studied (+/-)
Coolant Flow Rate	25%
Coolant Channel Area	25%
Coolant Inlet Temperature	25%
Internal Heat Generation	12.5%
Plate Thermal Conductivity	25%
Coolant Thermal Conductivity	25%
Plate Web Thickness	33%
MEA Thermal Conductivity	25%

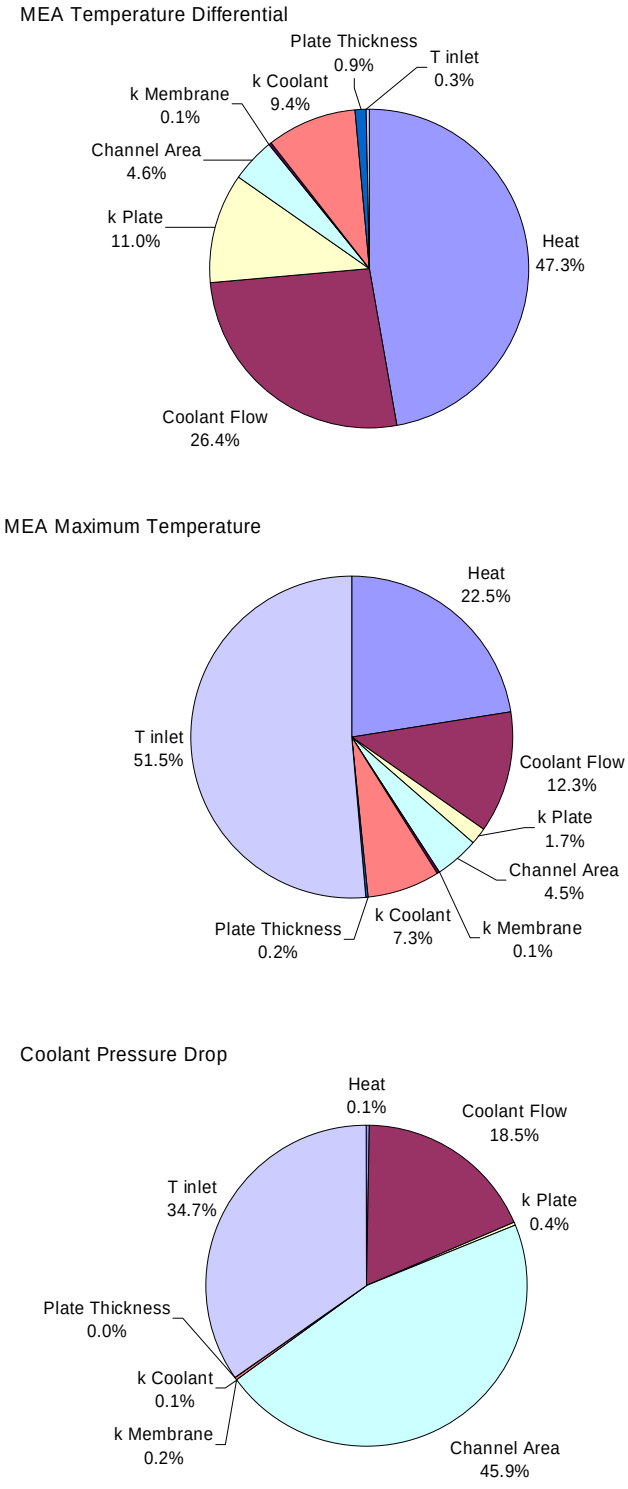

Figure 11. Results of sensitivity analysis

For the DOE study, a 2-level half-factorial DOE was combined with a 3-level Taguchi L-18 design. The total number of runs for this type of design is:

$$n_{factorial} = level^{(number\ of\ factors\ -\ fraction)} = 2^{(8-1)} = 128$$

$$n_{taguchi} = 18$$

$$n_{total} = 146$$

The maximum MEA temperature ($T_{max\text{-}MEA}$), the temperature differential across the MEA (dT_{MEA}), and the coolant channel pressure drop ($dP_{coolant}$) were evaluated as system responses. A sensitivity analysis was performed to reveal the relative impacts that each of the design parameters has on the system performance. Results of the sensitivity analysis are shown in Figure 11. The internal heat generation (Heat) and the coolant flow rate had the strongest effect on MEA temperature difference. Together, these two factors accounted for more than 70% of the dT_{MEA} response. The bipolar plate thermal conductivity (k Plate), coolant channel area, and the coolant thermal conductivity (k Coolant) together accounted for approximately 25% of the dT_{MEA} response. Aside from increasing the coolant flow rate and controlling the heat generation, bipolar plate materials with improved thermal conductivity, greater coolant channel surface area, and improved thermal conductivity were the most effective parameters for improving the temperature differential of the MEA. The maximum MEA temperature response was dominated by the coolant inlet temperature (T inlet), the heat generation, and the coolant flow rate. As expected, coolant pressure drop was dominated by coolant channel area, coolant inlet temperature, and coolant flow rate. Note that all the effects are based on the parameters selected and the range of values chosen for the DOE.

Finally, a probabilistic analysis was performed to determine the effect of variation of input load factors on thermal performance of a given design. The factors chosen for random input variables in this analysis included the heat generation rate, the inlet coolant temperature, and the coolant flow rate. Variation in these parameters is expressed as a normal distribution with a specified mean and standard deviation. Each parameter was allowed to vary a total of 5% (+/- 2.5% from the nominal design value). Figure 12 shows the distribution of the random input variables.

The parameters were then varied to develop a response surface of the performance parameters that included the maximum temperature of the MEA and the temperature differential across the MEA. The response surface was generated by running the parametric FEA thermal model with

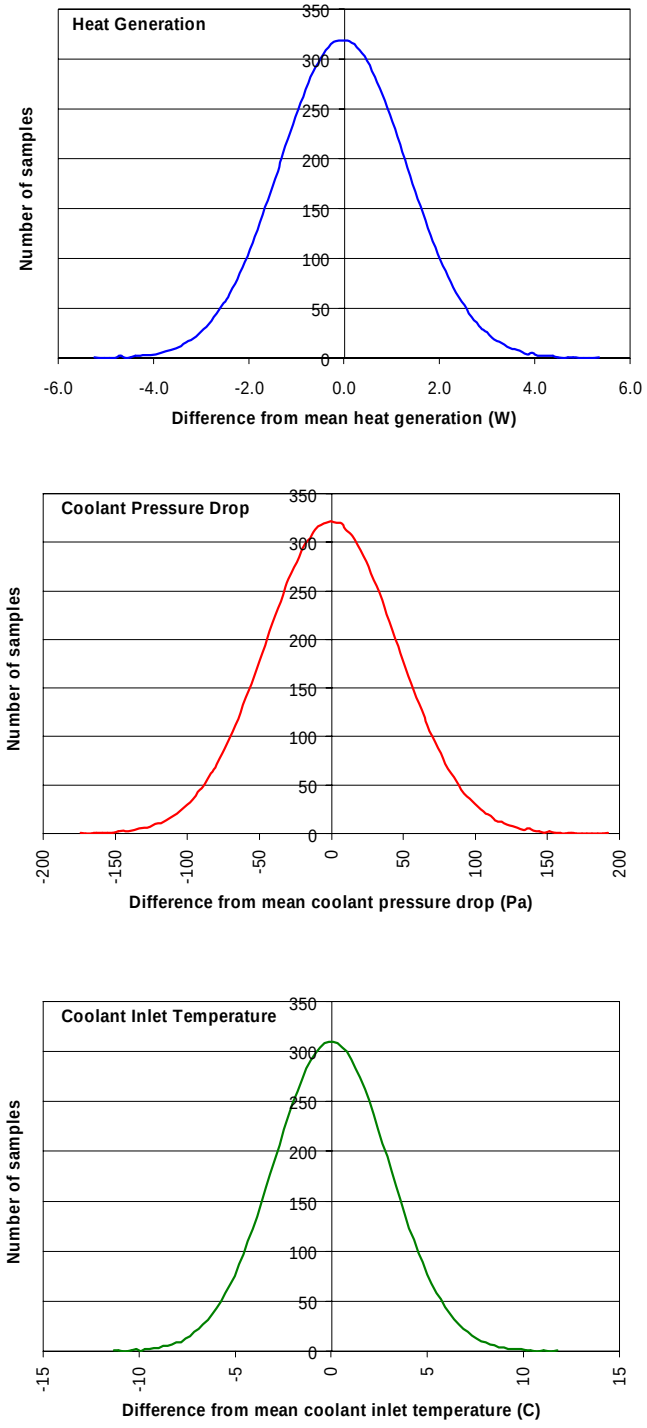

Figure 12. Distribution of random input variables

input boundary conditions sampled from the shown distributions using a central composite sampling technique.

For the case of three design parameters, the central composite method required 15 simulations to be run [(2)]. A forward step-wise regression model was then used to determine the response surface for each of the performance parameters ($T_{max\text{-}MEA}$ and dT_{MEA}). Once the response surface was generated and verified, 10000 samples of the output performance parameters were generated.

Figure 13 shows the correlation between the values extracted from the FEA and the values calculated from the dT_{MEA} response surface quadratic polynomial. This figure indicates a very good fit for the dT_{MEA} response surface. A "perfect" fit would have a slope of 1.0, y-intercept of 0.0, and an R^2 value of 1.0. A similar fit was achieved for $T_{max\text{-}MEA}$ response surface.

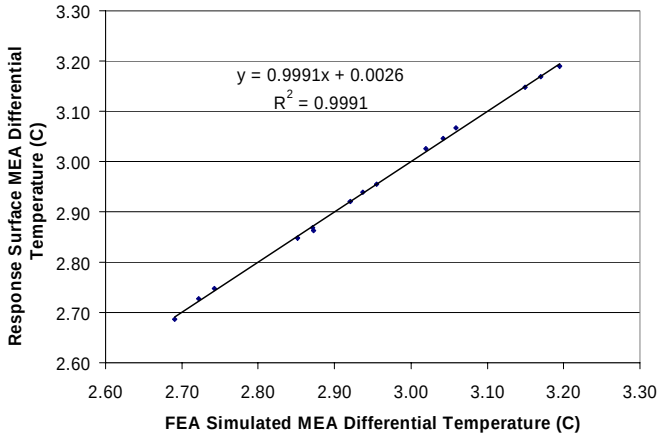

Figure 13. Correlation of FEA results and response surface

Figure 14 shows the distribution of $T_{max\text{-}MEA}$ and dT_{MEA} response to 10000 randomly varying values of heat generation, coolant pressure drop, and coolant inlet temperature. The dT_{MEA} response to 5% random variation in the input parameters was an average of 5.6ºC with a total range (maximum dT_{MEA}-minimum dT_{MEA}) of 0.4ºC, which is approximately 7% of the average response. Sensitivity analysis on the dT_{MEA} response showed that the response is primarily due to variations in the internal heat generation (66%). The inlet coolant pressure had the next greatest effect (18%), while the inlet coolant temperature accounted for 16% of the response. The $T_{max\text{-}MEA}$ response to 5% random variation in the input parameters was an average of 187ºC and a total range (maximum $T_{max\text{-}MEA}$ - minimum $T_{max\text{-}MEA}$) of 11.2ºC, which is approximately 6% of the average response. Sensitivity analysis on the $T_{max\text{-}MEA}$ response showed that the response is dominated by variations in the inlet coolant temperature (96%).

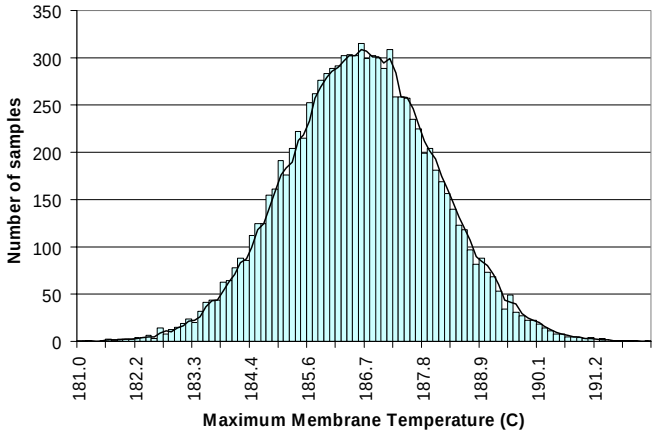

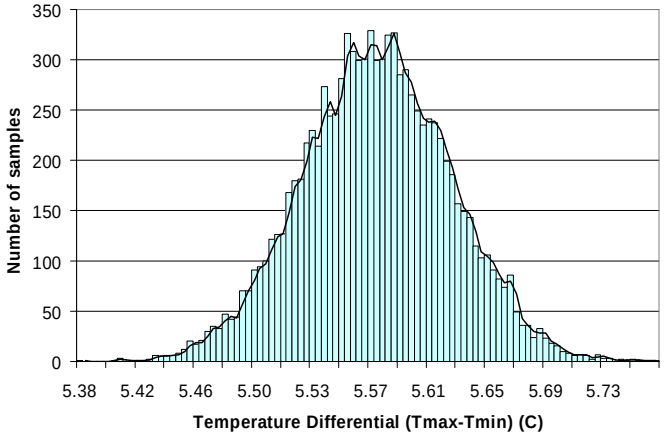

Figure 14. Distribution of output performance parameters

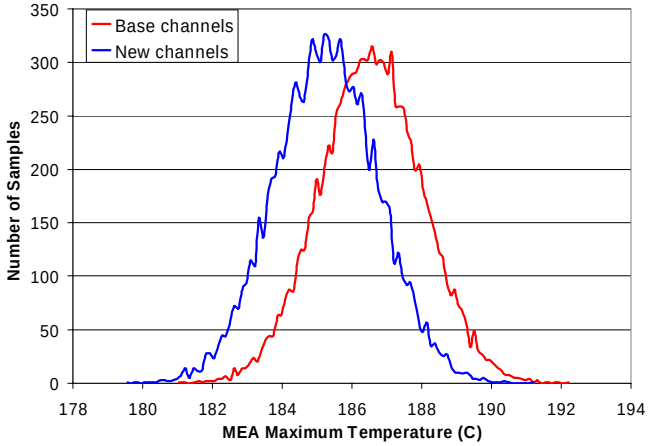

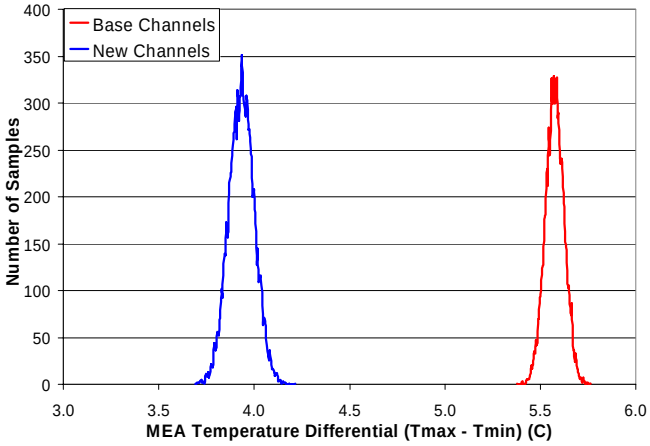

Figure 15. Comparison of output distributions for base and new channel designs

Figure 15 compares the output response distributions for the base coolant channel design and the new coolant channel design. This figure shows a substantially (30%) lower average dT_{MEA} for the new channel design (i.e., significantly lower temperature differential across the MEA). However, the new channel design showed a 35% increase in the standard deviation of dT_{MEA}. Although the temperature differential for the new design was lower, it was more sensitive to input load variations. The new channel design also exhibited slightly (0.8%) lower $T_{max\text{-}MEA}$ response, while the distribution of $T_{max\text{-}MEA}$ for the two designs was nearly identical.

CONCLUSIONS

The authors have developed a fuel cell stack thermal modeling process that incorporates a 3-D multi-cell stack thermal model, real-world geometry, integration with an external electrochemical model for predicting nonuniform heat generation, and integration with design space exploration and probabilistic design techniques.

The modeling process was demonstrated using Plug Power's high-temperature, PBI-based stack. Initial results showed how classic DOE techniques integrated with the model were used to define response surfaces and perform sensitivity studies on heat generation rates, fluid flow, bipolar plate channel geometry, fluid properties, and plate thermal material properties. The model showed nonuniform temperature distributions within the fuel cell stack that may cause degraded

performance, induce thermo-mechanical stresses, and be a source of reduced stack durability. NREL also used the model to propose an alternative coolant flow-path design that yields improved thermal performance. Elements from this analysis were recently incorporated into the latest Plug Power coolant flow-path design.

ACKNOWLEDGMENTS

This research effort was funded by the Department of Energy Office of Hydrogen Fuel Cells and Infrastructure Technologies. The authors would like to express their appreciation to Kathi Epping and Nancy Gardner of the Hydrogen, Fuel Cells & Infrastructure Technologies Program, and to William Ernst and Rhonda Staudt of Plug Power for their support on this project.

REFERENCES

1. ANSYS Inc. Probabilistic Design Techniques, Advanced Analysis Techniques Guide, August 2002.
2. Schmidt, R. and Launsby S., Understanding Industrial Designed Experiments, 4th edition, Air Academy Press, 2000.
3. Vlahinos A. and Kelkar S. "Body-in-White Weight Reduction via Probabilistic Modeling of Manufacturing Variations," *2001 International Body Engineering Conference*, SAE paper # 2001-01-3044, Detroit, MI, October 2001.
4. Vlahinos A. and Kelkar S. "Designing for Six-Sigma Quality with Robust Optimization Using CAE," *2002 International Body Engineering Conference*, SAE paper # 2002-01-2017, Paris, France, July 2002.
5. Vlahinos, A., Penney T., Kelkar S. "Engineering Quality into Digital Functional Vehicles," Proceedings of IDPS2002, *2002 Daratech Intelligent Digital Prototyping Strategies Conference*, Detroit, MI, June 2002.
6. Vlahinos A., Kelly K., Pesaran A., Penney T., "Empowering Engineers to Generate Six-Sigma Quality Designs," Proceedings of *First Annual Quality Paper Symposium, American Society for Quality, Automotive Division*, Livonia, MI, February 2003.